Laboratori Nazionali di Frascati

LNF-61/12 (1961)

G. Diambrini, A. S. Figuera, B. Rispoli, A. Serra: BREMSSTRAHLUNG SPECTRUM OF THE 1100 MeV ELECTRONSYNCHROTRON AT FRASCATI.

Estratto dal: Nuovo Cimento, 19, 250 (1961)

IL NUOVO CIMENTO Vol. XIX, N. 2 16 Gennaio 1961

Bremsstrahlung Spectrum of the 1000 MeV Electronsynchrotron at Frascati.

G. DIAMBRINI

C.N.R.N., Laboratori Nazionali - Frascati

A. S. FIGUERA (*), B. RISPOLI (**) and A. SERRA

C.N.R.N., Divisione Elettronica - Roma

(ricevuto il 26 Agosto 1960)

Summary. — The final results of some measurements on angular distribution and on Bremsstrahlung spectrum of the γ-ray beam of the Frascati electronsynchrotron are given. The experimental results of angular distribution for thick target fit with Schiff's theoretical angular distribution. We find, on the contrary, a difference between theory and experiments for thin target and this can be explained by multiple crosses through the target of the accelerated electrons. For the spectrum shape, comparing the experimental results with Bethe and Heitler's theory, we have that for thin target the experimental points are in fair agreement with the theoretical previsions while for thick target we find a difference in the high energy range and we see that this difference can be explained by many different reasons.

1. – Introduction.

In this paper definite results (1) about the bremsstrahlung spectrum of the 1000 MeV Frascati electronsynchrotron by using different targets and collimators are given.

(*) At present: Physics Department, University of Maryland.

(**) Comitato Nazionale per le Ricerche Nucleari and Istituto di Fisica dell'Università di Roma.

(1) The first results were given in *Nuovo Cimento*, 15, 500 (1960).

The subject of this experiment is to give a contribution to the understanding of the electronsynchrotron beam production mechanism, and to get useful results for research in photoproduction when using photons of an energy near to the upper limit of the spectrum.

Because the spectrum shape of the γ-ray beam depends essentially on the effective target thickness, on the collimation, on the energetic distribution of primary electrons and on possible multiple crossings through the target, it is necessary to determine the effective thickness of the targets in use, and the transmission factors of the collimators. So the angular distribution of the beam intensity for two different thicknesses of target are studied and the results, shown in Section 2, are compared with the theoretical angular distribution.

The experimental apparatus used for the bremsstrahlung spectrum measurements has been described in Section 3.

In Section 4 are given the spectra obtained by using 0.13 and 0.013 r.l. target thickness and, for each one of these, two collimators with acceptance angles of 3.6 and 0.75 mrad respectively.

In order that this paper may be useful to those wishing to measure spectrum with other similar accelerators there are some mathematical explanations in the Appendix.

2. – Beam angular distribution.

The experimental arrangement for the beam angular distribution measurement is shown in Fig. 1, where:

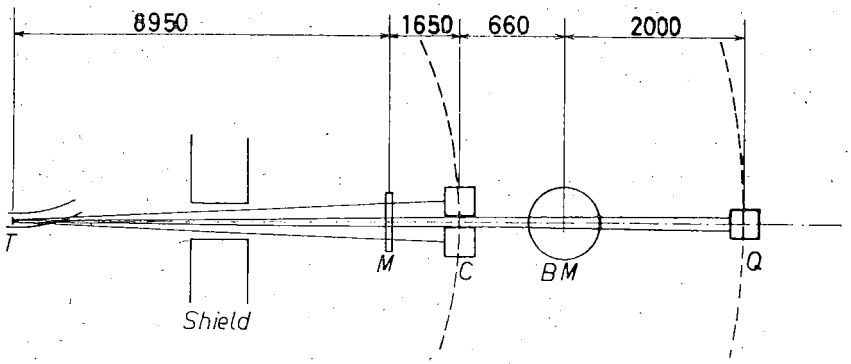

Fig. 1. – Experimental arrangement for angular distribution measurements. (Distances are given in millimeters).

T is the electronsynchrotron tantalum target;

M is an ionization chamber with thin aluminium walls and with electrodes of total thickness of $4.3 \cdot 10^{-4}$ r.l.;

C is a lead collimator (collimators with hole diameters of 5 mm and 2 mm corresponding to angular openings 0.47 and 0.19 mrad respectively, were used);

BM is a « sweep » magnet in the gap of which there is a field of about 15 kG able to sweep aside all charged particles travelling with the beam;

Q is a total absorption chamber of the type described by WILSON [2].

The distance of 2 m between BM and Q ensures that any charged particles travelling with the beam and being deflected by BM, will not impinge upon the chamber Q and affect the ionization measurements. The collimator C and the chamber Q are placed on movable bases which can be moved azimuthally about the centre T.

The chamber M, crossed by the whole beam, has been used in order to be able to refer to the same charge m, the measurements taken at several angles. Charges q collected in Q by the beam portion crossing C, and charges m collected in M, are measured by integrators connected to ionization chambers.

The angular distribution of beam intensity defined by

$$I(\theta) = \frac{q(\theta)}{m},$$

is obtained by moving the collimator C and the chamber Q about the centre T at an angle θ. By following this method, measurements in steps of 0.5 mrad were made with tantalum targets of 0.5 and 0.05 mm in thickness respectively equal to 0.13 and 0.013 r.l. Each measurement has been repeated at least four times.

The measurements with 0.13 r.l. target were made with a 5 mm hole collimator C, *i.e.* with a 0.47 mrad angular opening and by taking as charge unity $m = 1.2 \cdot 10^{-6}$ C.

The experimental results are shown in Fig. 2 together with the theoretical angular distribution, computed by using Schiff's formula [3]

$$\frac{I(\theta)}{I_0} = \frac{Ei(-\theta^2/2\beta x)}{\ln 2\beta x E^2 - C},$$

where Ei is the exponential integral function [4], β is a function depending on the energy E (expressed in units of mc^2) of the electrons striking the target

---

[2] R. R. WILSON: *Nucl. Instr.*, 1, 101 (1957).
[3] L. I. SCHIFF: *Phys. Rev.*, 70, 87 (1946).
[4] E. JANKE and F. EMDE: *Tables of Functions* (New York, 1945).

and on the target material and thickness x (expressed in cm), $C = 0.577\,2$ is the Euler constant.

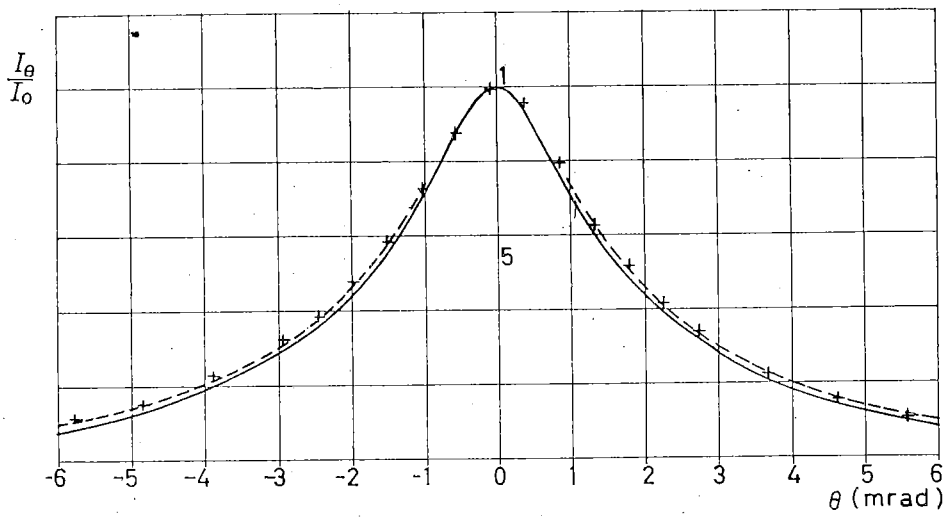

Fig. 2. – Angular distribution. —— Schiff theoretical angular distribution for 0.13 r.l. target; – – – Schiff theoretical angular distribution for 0.156 r.l. target; + experimental points for 0.13 r.l. target.

The continuous curve refers to the 0.5 mm (0.13 r.l.) thick target while the dashed curve was calculated for the 0.6 mm (0.156 r.l.) thick target to take into account that the target is inclined at approxymately 30° to the direction of the electron beam, making the effective target thickness 0.6 mm. So it was confirmed that the thickness contributing to the radiation is in effect the true thickness.

The 0.013 r.l. target measurements were made by using a collimator C having a 2 mm diameter hole *i.e.* a 0.19 mrad angular opening, taking as charge unity $m = 4 \cdot 10^{-7}$ C. The experimental results are shown in Fig. 3 together with the Schiff theoretical distribution, calculated for a 0.05 mm (0.013 r.l.) target thick-

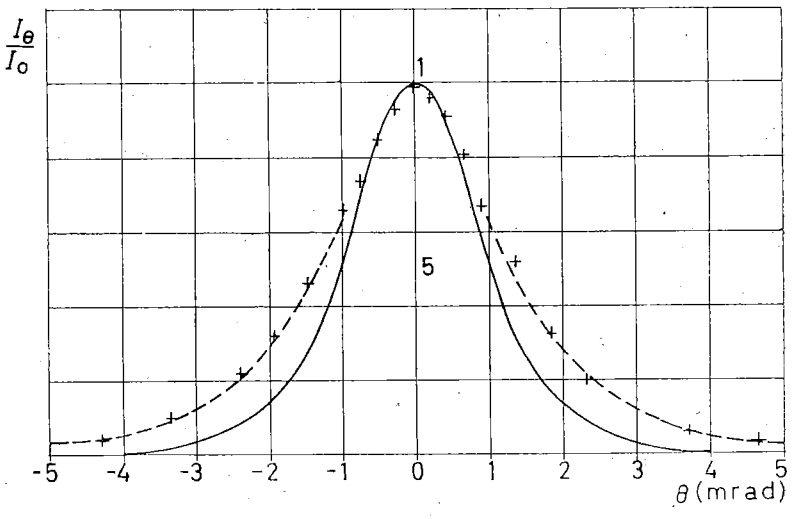

Fig. 3. – Angular distribution. —— Schiff theoretical angular distribution for 0.013 r.l. target; – – – Schiff theoretical angular distribution for 0.039 r.l. target; + experimental points for 0.013 r.l. target.

ness as shown by the continuous curve. It can be seen that there is a discrepancy between theoretical curve and experimental results which fit the theoretical distribution (dashed curve) calculated for a 0.15 mm (0.039 r.l.) target thickness.

It can be deduced then that the target has an effective thickness, contributing to the radiation, greater than the actual thickness.

This phenomenon can be explained qualitatively (5) by examining the effect of multiple crossings of electrons through the target. In fact if we consider only the ionization energy losses, about 100 keV, for each crossing of the target, and as the width of the target is 4.5 mm, electrons can only cross the target three times before attaining a new orbital equilibrium.

This gives the same effect as electrons crossing once a target of three times the actual target thickness.

3. – Experimental apparatus used for the bremsstrahlung spectrum measurements.

The experimental arrangement for the bremsstrahlung spectrum determination is shown in Fig. 4 where:

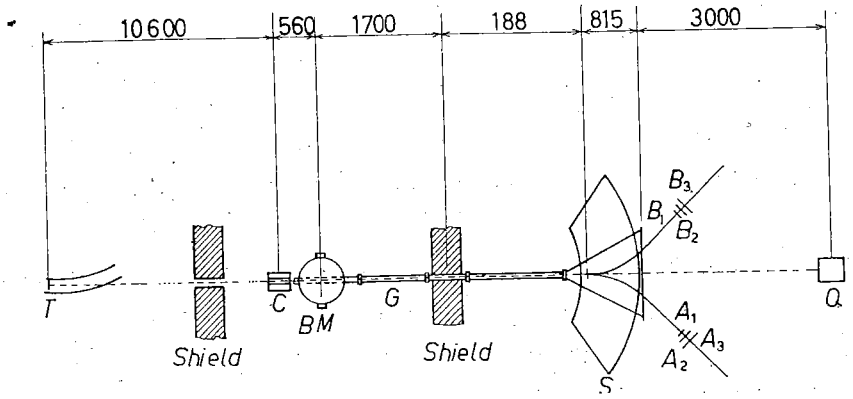

Fig. 4. – Experimental arrangement for bremsstrahlung spectrum measurements. (Distances are given in millimeters).

T is the tantalum target (with a thickness: $s_1 = 0.13$ or $s_2 = 0.013$ r.l.) of the electronsynchrotron;

C is a lead collimator 30 cm in lenght. Two collimators were used, one having a central hole diameter of 38 mm giving an accepted angle of 3.6 mrad, and the other having a central hole diameter of 8 mm, giving an acceptance angle of 0.75 mrad;

(5) A correct quantitative explanation requires the study of very low energy photon losses.

BM is the « sweep » magnet, in the gap of which there is a field of 15 kG;

G is a tube evacuated to a pressure of 0.03 mm Hg which is connected at one end to the chamber of the spectrometer;

S is an electron pair spectrometer (6);

R is the spectrometer radiator, made of an aluminium disc 6 cm in diameter and $1.08 \cdot 10^{-3}$ r.l. thick;

Q is a monitor formed by a total absorption quantameter (2);

A_1, A_2, A_3 and B_1, B_2, B_3 are two scintillation counter telescopes placed so that they can detect only the symmetric pairs of electrons.

The beam, collimated by C, enters the tube G after being « cleaned » by the sweep magnet, then it is completely absorbed by the monitor Q after crossing the radiator R in which the electron pairs are produced.

The input of the vacuum tube G and the output end of the vacuum chamber of the spectrometer are sealed with 0.2 mm thick mylar foil.

The counter telescopes detect the symmetric pairs having an energy E function of field B in the spectrometer gap. The energy K of the γ-ray producing pair is given by $K = 2E$ neglecting the rest mass of the two electrons.

The energy selection is obtained by changing the magnetic field value in the spectrometer gap from 0.5 to 10.5 kG. In this manner the two counter telescopes, that are in a fixed position, can detect the electron symmetric pairs in the energy range from 25 MeV to 525 MeV. So it is possible to examine the full spectrum of γ-rays.

In order to determine the position of the telescopes, the electron trajectories were determined by means of an electronic computer and controlled experimentally by the floating wire technique.

The spectrometer magnet current supply had a stability of ± 0.1 per cent. The electron trajectories were determined with a precision of ± 0.3 per cent The spectrometer is previously calibrated by determining the behaviour of the field intensity as function of the magnet current. For any value of the magnetic field there is a determined electron energy for the electrons crossing the two telescopes. So it is possible to express the electron energy as a function of the magnet current.

The current is measured with a precision of 0.1 per cent by a comparison method using a precision potentiometer and a standard cell.

As the width of the first counter of each telescope is 18 mm, by the spectrometer optics (6) the percentage interval of the energy accepted by the telescopes $\Delta E/E = 2.7$ per cent is obtained. The successive counter dimensions of each

(6) G. BOLOGNA, G. DIAMBRINI, A. S. FIGUERA, U. PELLEGRINI, B. RISPOLI, A. SERRA and R. TOSCHI: Internal note no. 17 of Laboratori Nazionali di Frascati (Sept. 28, 1959) to be published in *Nucl. Instr. and Methods*.

telescope were increased in order to avoid counting losses due to the electron scattering. The first scintillator height is 54 mm. All the scintillators are of 1 mm plastic.

Fig. 5 shows the block diagram of the electronic apparatus used for the bremsstrahlung spectrum measurements.

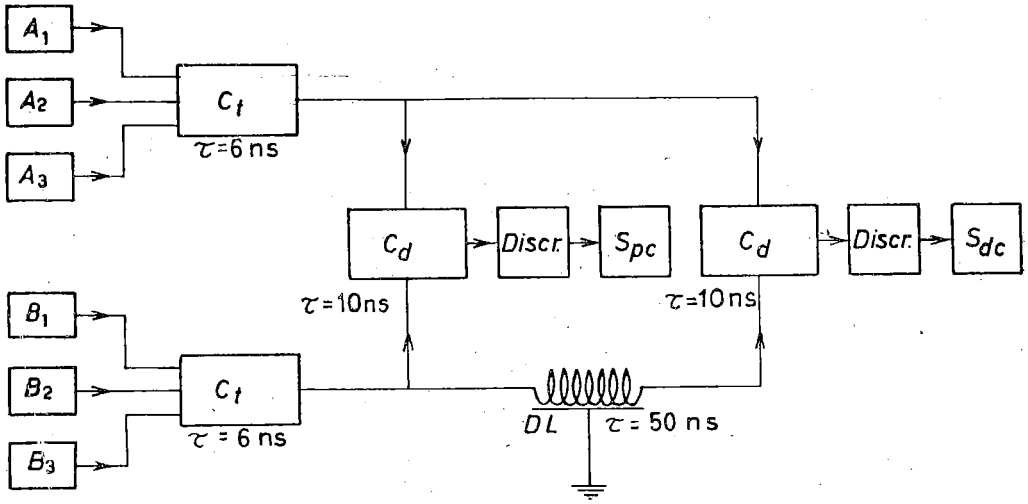

Fig. 5. – Electronics block diagram.

The photomultiplier anodes of the three counters of each telescope are connected to a three-fold coincidence circuit C_t with a resolution time of $\tau = 6$ ns. The outputs of the two three-fold coincidences C_t go to two two-fold coincidence circuits C_d with $\tau = 10$ ns directly to the first, and to the second through a delay DL of 50 ns.

The two-fold coincidences are followed by a discriminator and a scaler. It is possible to record simultaneously the prompt S_{pc} and delayed coincidence S_{dc}.

Knowing the delayed coincidence it is possible to calculate true coincidences due to symmetric pairs produced in the aluminium radiator by making the difference $S = S_{pc} - S_{dc} - B$, where $B = B_p - B_d$ is the difference between the prompt and delayed coincidences when the spectrometer radiator R is removed.

Measurements of the difference S as a function of the electron energy were made by varying the magnet current and by referring each measurement to the same charge $q = 3 \cdot 10^{-6}$ C collected in the monitor Q which corresponds to about $1.4 \cdot 10^{10}$ equivalent quanta crossing the radiator R. The measurements for each energy were repeated several times in order to have a statistical error of less than 1 per cent.

This was possible without prolonging the measurement time in view of the electronsynchrotron's high beam intensity. Even when a collimator of 0.75 mrad

is used an average intensity of $6 \cdot 10^9$ equivalent quanta per minute is obtained after the collimator.

The γ-beam intensity was maintained, during the measurement, at a level (below the maximum in the case of a 3.6 mrad collimator) so that also for the low energy range of the spectrum, the ratio $\eta = S_{ac}/S$ was less than 5 per cent. In fact because of the high resolution power of the coincidence circuits the maximum contribution to chance coincidences is given by the coincidences due to two asymmetric pairs, each one of these having an electron of energy equal to E.

The ratio between spurious coincidences and true coincidences is given by

$$\eta = 8\tau \frac{Y}{T}\left(1 - \frac{E}{K_{\max}}\right)^2,$$

where τ is the resolution time of the coincidence circuit, T is the length of the pulse of the electrosynchrotron γ-ray beam, $K_{\max}$ is the maximum energy of photons, E is the electron energy and

$$Y = \Phi_{\text{tot}} s N_e \frac{A \varrho X}{P},$$

where: Φ_{tot} is total cross section for the production of pairs; s is the thickness in r.l. of the electronsynchrotron target; N_e is the number of primary electrons striking the target; A is the Avogadro number; ϱ is the density (g/cm^3) of the spectrometer radiator; X is the spectrometer radiator thickness (cm); P is the spectrometer radiator atomic weight.

Then it can be seen that η is maximum when the energy is low and it is directly proportional to the intensity $N_e s/T$ of the γ-ray beam.

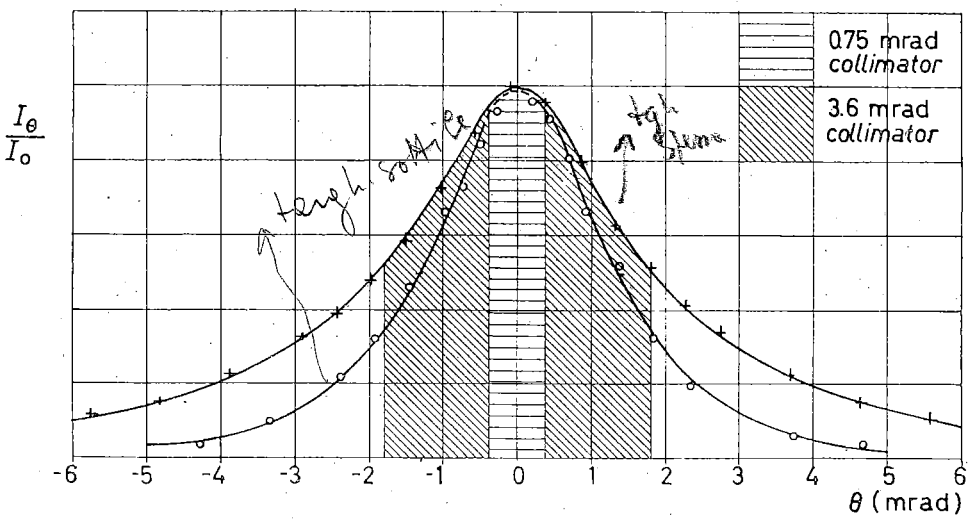

Fig. 6. – Diagram of the transmission factors of the collimators.

The 8 mm collimator (angular opening 0.75 mrad) has a transmission factor of 1.3 per cent and 3.2 per cent using respectively 0.13 and 0.013 r.l. targets.

The 38 mm collimator (angular opening 3.6 mrad) has transmission factors of 20 per cent with the 0.13 target and of 42.5 per cent with the 0.013 r.l. target.

The transmission factors defined by the ratio between the transmitted intensity and the incident intensity were calculated by the experimental angular distributions shown in Fig. 6.

4. – Experimental results of the bremsstrahlung spectrum measurements.

Let us define now the function « intensity of the bremsstrahlung » $I(u)$ given by

$$I(u) = KN(K)\frac{q^* E_0}{q}, \tag{1}$$

where $u = K/E_0$, $E_0 = 1000$ MeV maximum energy of primary electrons and $N(K)$ is the number of photons having energy $K = uE_0$.

Monitor Q gives an integral information of the energy transmitted by the beam by collecting the electric charge

$$q = q^* \int_0^{E_0} KN(K)\,\mathrm{d}K,$$

corresponding to q/q^* MeV of irradiated energy, $q^* = 2.07 \cdot 10^{-19}$ C/MeV being a characteristic constant of the instrument.

The number $S = S_{pc} - S_{dc} - B$ of symmetric pairs of electrons is given by

$$S = N(K)\,\Delta K r \left[\sigma_p\left(K, \frac{1}{2}\right) + \sigma_t\left(K, \frac{1}{2}\right)\right]\frac{\Delta E}{K},$$

where: $\sigma_p(K, \frac{1}{2})$ and $\sigma_t(K, \frac{1}{2})$ are respectively the cross-sections of the production of symmetric pairs in the field of the nucleus corrected for the Born approximation ([7,8]) and in the field of the electron ([9]); r is the number of atoms per cm² of spectrometer radiator; $\Delta E = \Delta K/2$ is the energy spread of electrons accepted by the scintillators.

([7]) H. BETHE and W. HEITLER: *Proc. Roy. Soc.*, A **146**, 83 (1934).

([8]) H. DAVIES, H. A. BETHE and L. C. MAXIMON: *Phys. Rev.*, 93, 788 (1934).

([9]) J. A. WHEELER and W. E. LAMB: *Phys. Rev.*, **55**, 858 (1939); **101**, 1836 (1956).

From the expressions (1) and (2) we can obtain

$$I(u) = \frac{2q^* E_0}{rq} \frac{S}{[\sigma_p(K, \frac{1}{2}) + \sigma_t(K, \frac{1}{2})](\Delta K/K)^2} .$$

Particularly for two selected energies $K = K_0$ and $K = K_n$ we have

$$\frac{\Delta K_0}{K_0} = \frac{\Delta K_n}{K_n} , \qquad q_0 = q_n , \qquad q_0^* = q_n^* .$$

so that

$$\frac{I_n}{I_0} = \frac{S_n}{S_0} \frac{\sigma_p(K_0, \frac{1}{2}) + \sigma_t(K_0, \frac{1}{2})}{\sigma_p(K_n, \frac{1}{2}) + \sigma_t(K_n, \frac{1}{2})} .$$

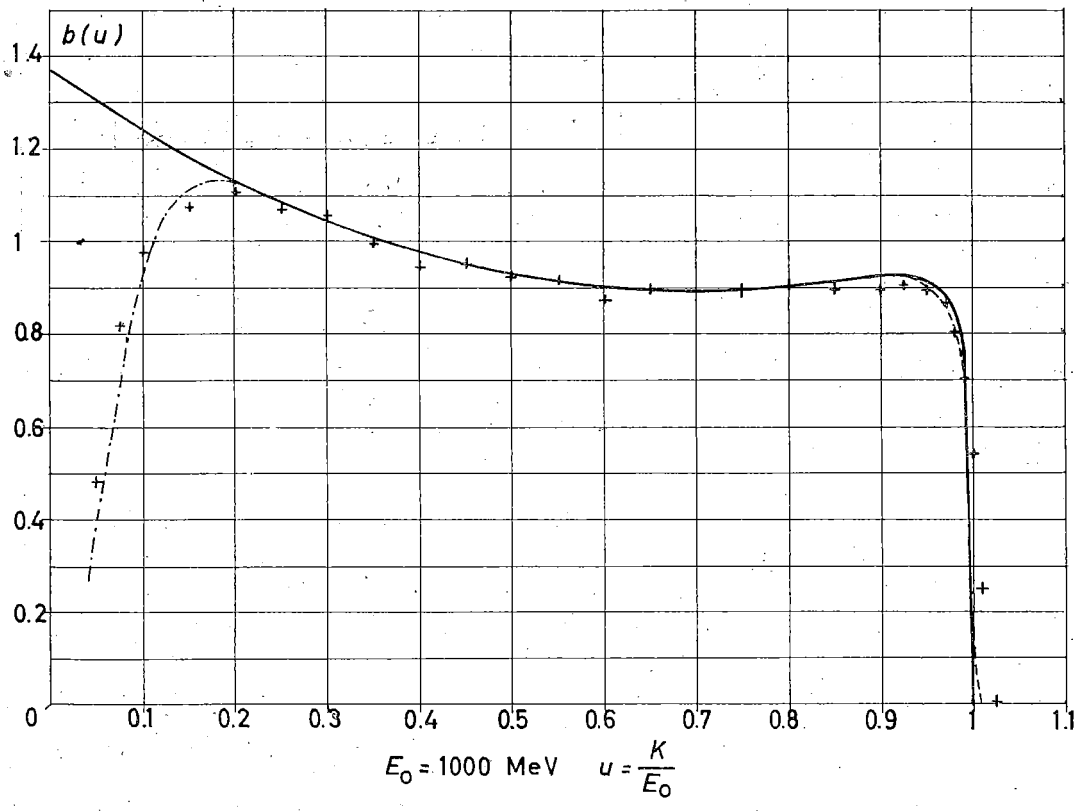

Fig. 7. – Bremsstrahlung spectrum of 0.013 r.l. target and 0.75 mrad collimator. —— Theoretical (BETHE and SALPETER); –·–·– theoretical, corrected for the scattering in the radiator and for the vertical dimension of the scintillators; – – – theoretical, corrected for the resolution function of the detecting apparatus.

In Fig. 7, 8, 9 are shown the experimental results of the ratio I_n/I_0 with the statistical error (less than 1 per cent) as function of $u = K/E_0$, by assuming $K_0 = 700$ MeV. These experimental results were compared with the theo-

retical behaviour (continuous curve) given by the expression:

$$b(u) = \frac{K(\sigma_n + \sigma_{el})}{\int_0^1 K(\sigma_n + \sigma_{el})\,du},$$

which is the value of the intensity of the bremsstrahlung normalized at the unit area. In this expression σ_n and σ_{el} are respectively the cross-sections for bremsstrahlung in the field of the nucleus corrected for the Born approximation ([7,10]) and in the field of the electron ([9]).

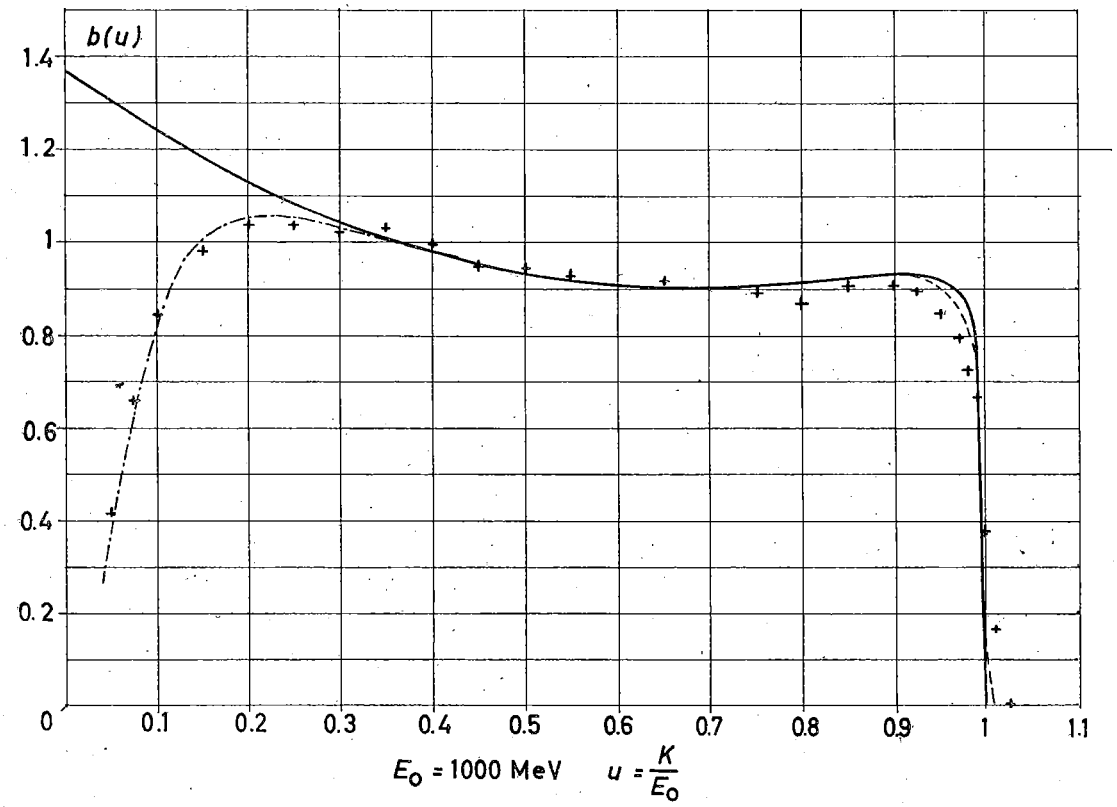

Fig. 8. – Bremsstrahlung spectrum of 0.013 r.l. target and 3.6 mrad collimator. —— Theoretical (BETHE and SALPETER); –·–·– theoretical, corrected for the scattering in the radiator and for the vertical dimension of the scintillators; – – – theoretical, corrected for the resolution function of the detecting apparatus.

The dashed curve that departs from the continuous curve in the low energy range of photons was obtained by subtracting from the theoretical curve the counting losses due to the scattering of electrons in the radiator and to the vertical dimension of the scintillators (see Appendix).

([10]) H. OLSEN: *Phys. Rev.*, 99, 1335 (1955).

The dashed curve shown in the range of the high energy spectrum, is obtained by averaging the theoretical curve on the triangular resolution of the detecting apparatus.

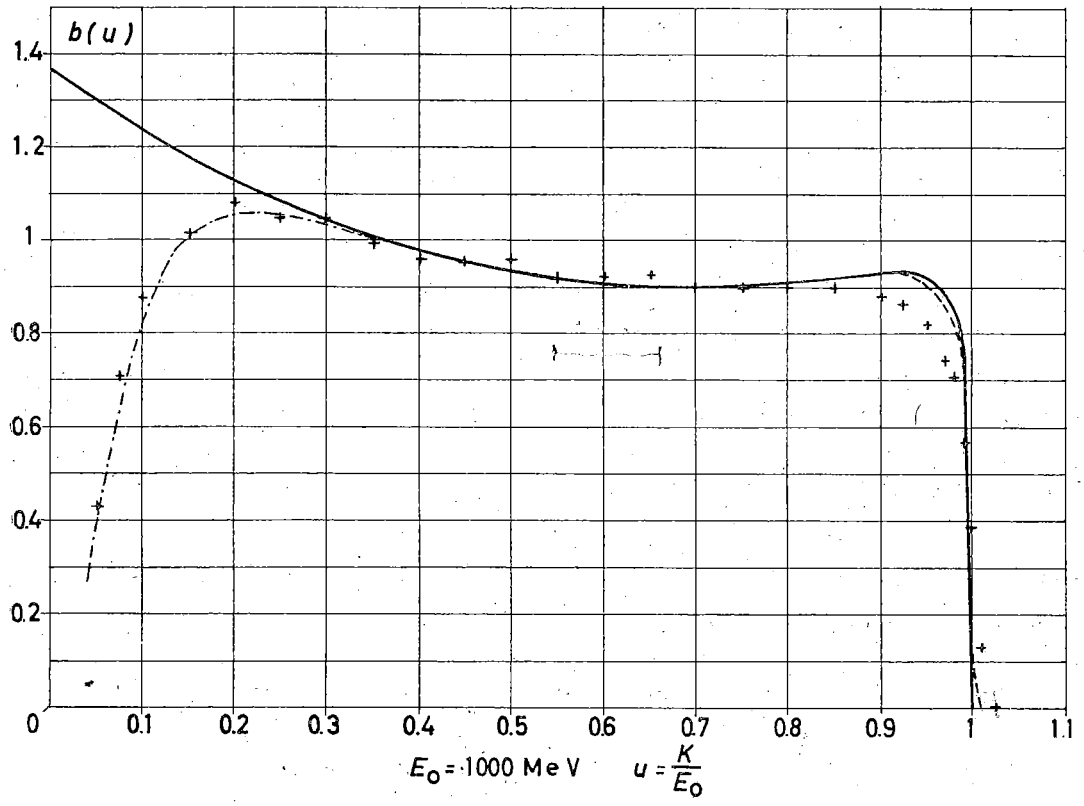

Fig. 9. – Bremsstrahlung spectrum of 0.13 r.l. target and 3.6 mrad collimator. —— Theoretical (BETHE and SALPETER); –·–·– theoretical, corrected for the scattering in the radiator and for the vertical dimension of the scintillators; –/–/– theoretical, corrected for the resolution function of the detecting apparatus.

One can see how the experimental results fit within the limits of 2 per cent with the theoretical curve in Fig. 7 corresponding to the 0.013 r.l. target and to a collimator with a transmission factor of 3.2 per cent while they do not fit when a collimator with a transmission factor of 42.5 per cent is used (Fig. 8), and they move even further away when a 0.13 r.l. target with a collimator transmission factor of 20 per cent are used (Fig. 9). Another series of measurements made with a 0.13 target and a transmission factor of 1.3 per cent (not shown) are equal (within the experimental tolerance) to the results shown in Fig. 9.

This discrepancy in the high energies range is principally due to:

a) the electrons crossing target may irradiate a high energy photon after irradiating one ore more of very low energy because of the target thickness;

b) the effects of collimation together with scattering in the target;

c) the energy fluctuations of the electrons striking the target.

The effect of the target thickness can easily be seen by comparing the experimental results, for $u > 0.8$ shown in Fig. 7 and 8 at the thin target with results of Fig. 9 at the thick target.

For the collimator effects, it can be said that if the beam is collimated there are no accepted large angle photons generated which are generally obtained by electrons that penetrate more deeply before irradiating (the natural emission angle of photons is ~ 0.5 mrad). In fact by the examination of the data obtained using the same thin target but different collimators, it is possible to see (Fig. 7 and 8) that there is a loss of high energy photons using collimators with larger acceptance angles; however this effect is negligible below a certain value of the acceptance angle of the collimator because of the shape of the function I_0/I_0 shown in Fig. 6.

The effect of point *c*) contributes less than the others to the deformation of the spectrum.

In conclusion we can see from Fig. 7 that the energy spread of electron-synchrontron electrons produces deviations in the high energy range of the spectrum less than 2 per cent.

Appendix

Calculation for determining the counting losses due to vertical deviation scattering of electrons in the radiator of the spectrometer.

If we consider a projection in a vertical plane passing through the axis of the γ-ray beam, the angular distribution of the electrons which have crossed a radiator of thickness δ is:

$$P(\theta)\,\mathrm{d}\theta = \frac{1}{\sqrt{2\pi}\theta_M} \exp\left[-\frac{1}{2}\left(\frac{\theta}{\theta_M}\right)^2\right]\mathrm{d}\theta\,.$$

where $\theta_M(16/E)\sqrt{\delta}$ and $P(\theta)\,\mathrm{d}\theta$ is the probability that the direction of an electron is between θ and $\theta + \mathrm{d}\theta$.

The probability for a positive electron to be generated in $\mathrm{d}\theta^+$ and for negative electron in $\mathrm{d}\theta^-$ simultaneously is then:

$$P(\theta^+, \theta^-)\,\mathrm{d}\theta^+\,\mathrm{d}\theta^- = \frac{1}{2\pi\theta_M^+\theta_M^-} \exp\left[-\frac{1}{2}\left(\frac{\theta^+}{\theta_M^+}\right)^2\right] \exp\left[-\frac{1}{2}\left(\frac{\theta^-}{\theta_M^-}\right)^2\right]\mathrm{d}\theta^+\,\mathrm{d}\theta^-,$$

If the electrons of a pair are detected by two detectors $2\,h$ in height placed at a distance s from the radiator (measured along the trajectory), we can write

the probability $I(\delta, z)$ of detecting an electron pair that has been generated at a point of vertical co-ordinate z (the origin of the co-ordinate is at the center of the radiator) and has passed through a thickness δ as:

$$I(\delta, z) = \frac{1}{2\pi\theta_M^+\theta_M^-}\int_{\theta_1^+}^{\theta_2^+}\exp\left[-\frac{1}{2}\left(\frac{\theta^+}{\theta_M^+}\right)^2\right]\mathrm{d}\theta^+\int_{\theta_1^-}^{\theta_2^-}\exp\left[-\frac{1}{2}\left(\frac{\theta^-}{\theta_M^-}\right)^2\right]\mathrm{d}\theta^-,$$

θ_1^+, θ_1^-, θ_2^+, θ_2^- are the limit angles (functions of h and z) accepted by the detectors for electron pairs generated at a point of the radiator of co-ordinate z.

For the probability of detecting an electron pair emitted from an arbitrary point between 0 and z_0, which has to pass through the thickness δ of the radiator, we have:

$$W(\delta) = \frac{\int_0^{z_0} N(z)\, I(\delta, z)\,\mathrm{d}z}{\int_0^{z_0} N(z)\,\mathrm{d}z}, \tag{A.1}$$

where $N(z)$ is the probability that the pairs are generated at the height z.

We consider $N(z) = \text{const}$ because in the first approximation the intensity distribution of the γ-ray beam on the radiator surface is constant. Let us neglect successive integration on the thickness, because of the assumption that all electrons do pass through the thickness $\delta_0/2$ (in our case we have $\delta_0 = 1.08 \cdot 10^{-3}$ r.l.).

By these simplifications we may express the relation (A.1) by:

$$W\left(\frac{\delta_0}{2}\right) = \frac{1}{z_0}\int_0^{z_0} I\left(\frac{\delta_0}{2}, z\right)\mathrm{d}z\,.$$

We can resolve graphically this integral.

Considering the symmetric pairs only we have

$$E^+ = E^- = E; \qquad \theta_M^+ = \theta_M^- = \theta_M = \frac{16}{E}\sqrt{\frac{\delta_0}{2}}; \qquad \frac{\theta^+}{\theta_M^+} = \frac{\theta^-}{\theta_M^-} = t\,,$$

$$\theta_1^- = \theta_1^+ = \theta_1; \qquad \theta_2^- = \theta_2^+ = \theta_2; \qquad x_1 = \frac{\theta_1}{\theta_M}; \qquad x_2 = \frac{\theta_2}{\theta_M}.$$

Then:

$$I\left(\frac{\delta_0}{2}, z\right) = \frac{1}{\sqrt{2\pi}}\int_{x_1}^{x_2}\exp\left[-\frac{t^2}{2}\right]\mathrm{d}t\,,$$

that is a tabulated integral.

Integrating the equation by KERST and SERBER ([11]), we can obtain the expression of the limit angles as a function of the z co-ordinate and of height $2h$ of the detectors ([6]). We have:

$$\theta_{1,2} = \frac{1}{V_{12}}[\pm h - V_{11} z] .$$

In this equation V_{11} is the linear vertical enlargement, that is the ratio between the arrival height at the detector and the departure height from the radiator of an electron which has at the beginning a zero angle with the spectrometer axis. The quantity V_{12} is the ratio between the arrival height at the detector and the departure angle at the radiator projected on the vertical plane passing through the spectrometer axis, of an electron that leaves the centre of the radiator.

The quantities V_{11}, V_{12} were determined by using the floating wire technique. We obtain the values:

$$\theta_{1,2} = [\pm 11.61 - 0.30 \cdot z] \text{ mrad} .$$

Then for each value of z we have the two integration limits for the integral: $I(\delta_0/2, z)$.

([11]) D. W. KERST and R. SERBER: *Phys. Rev.*, **60**, 53 (1941).

RIASSUNTO

Vengono dati i risultati finali di una serie di misure sulla distribuzione angolare e sullo spettro di bremsstrahlung dell'elettrosincrotrone di Frascati. I risultati sperimentali di distribuzione angolare per un convertitore spesso coincidono con la distribuzione teorica di Schiff mentre per un convertitore sottile si ha una discrepanza che può essere spiegata come effetto di attraversamenti multipli del convertitore del sincrotrone da parte degli elettroni accelerati. Per la forma dello spettro, dal confronto dei dati sperimentali con l'andamento previsto da Bethe e Heitler si ha che per convertitore sottile l'andamento sperimentale coincide abbastanza bene con l'andamento teorico mentre con convertitore spesso si nota una discrepanza nella regione ad alta energia, discrepanza che si vede può essere dovuta a diverse cause.